Symmetrized holographic entropy cone

Matteo Fadel[1,*] and Sergio Hernández-Cuenca[2,†]
[1]*Department of Physics, ETH Zürich, 8093 Zürich, Switzerland*
[2]*Department of Physics, University of California, Santa Barbara, California 93106, USA*

(Received 15 December 2021; accepted 4 March 2022; published 11 April 2022)

The holographic entropy cone (HEC) characterizes the entanglement structure of quantum states which admit geometric bulk duals in holography. Due to its intrinsic complexity, to date it has only been possible to completely characterize the HEC for at most $n = 5$ parties. For larger n, our knowledge of the HEC falls short of incomplete: almost nothing is known about its extremal elements. Here, we introduce a symmetrization procedure that projects the HEC onto a natural lower dimensional subspace. Upon symmetrization, we are able to conjecture precise properties that its extremal structure exhibits for general n. Further, by applying this symmetrization to the quantum entropy cone, we are able to quantify the typicality of symmetrized holographic entropies, which we find to be exponentially rare quantum entropies in the number of parties.

DOI: 10.1103/PhysRevD.105.086008

I. INTRODUCTION

From the microscopic degrees of freedom of gravity to the macroscopic emergence of spacetime itself, the holographic principle has provided deep insight into many aspects of quantum gravity [1,2]. Realizations thereof like AdS/CFT [3,4] may be used to define a bulk theory of quantum gravity nonperturbatively in terms of a lower-dimensional boundary field theory—a hologram. Elucidating quantum gravity then amounts to decoding the holographic dictionary between bulk and boundary physics. A remarkably powerful entry in this dictionary concerns the correspondence between boundary entanglement and bulk geometry, and is often captured by the slogan that spacetime emerges from entanglement [5].

At the heart of this idea lies the Ryu-Takayanagi (RT) formula [6] (see [7–9] for generalizations thereof), which geometrizes the von Neumann entropy of boundary regions into areas of certain surfaces in the bulk. By RT, the emergence of a classical spacetime from entanglement relies on strong constraints on the entanglement structure of boundary states: only so-called holographic states with certain patterns of quantum entanglement admit such geometrizations. When formulated as inequalities for the von Neumann entropy, these constraints define a polytope in the space of entropies of all subsystems one can form involving n parties. In [10], this object was proven to be a rational polyhedral cone for any given n and coined the holographic entropy cone (HEC). The work of [10] also pioneered a graph-theoretic reformulation of RT entropies, later formalized by [11], that made the HEC amenable to systematic study. In particular, [10] proved that the HEC could be equivalently defined as the space of entropies that can be realized by the weights of minimum cuts on weighted graphs. Despite this breakthrough, deciphering the general structure of the HEC_n for general n remains a formidable challenge: its complete description is only known for up to $n = 5$ parties [12], and despite the systematic computational algorithms of [11] for arbitrary n, results for $n \geq 6$ are only partial and highly incomplete [10,13].

The remarkably complicated structure the HEC_n exhibits as n increases suggests that an explicit description of all its rich details, if attainable at all, would probably not be very illuminating. Hence, rather than trying to explicitly describe the HEC in full glory, some attempts at studying it have focused on trying to understand its basic structural properties [14–18]. In pursuing the latter strategy, the present work identifies an interesting projection of the HEC which is able to wash out its uninteresting fine details while preserving nontrivial features of the extremal structure of the HEC_n at arbitrary n. Since this projection is inspired by the underlying symmetries of the HEC, we will be referring to it as a symmetrization. Similar approaches have been extremely successful in the context of Bell nonlocality, where a projection of the local polytope onto the subspace invariant under permutation of the particles allowed to find Bell inequalities valid for arbitrary n [19,20]. Importantly, our symmetrization of the HEC seems to take a simple enough form that we are able to propose a general solution to it, and thereby conjecture nontrivial properties that all extreme rays and facets of the HEC_n must satisfy for all n.

*fadelm@phys.ethz.ch
†sergiohc@ucsb.edu

We begin in Sec. II with a brief review of basic quantum and holographic inequalities that will be appear throughout, and a self-contained introduction to the graph models of holographic entanglement of [10]. Having laid out our notation, in Sec. III we then carefully explain the symmetrization operations that are central to our explorations. Section IV presents our explicit results and conjectures for the general form of the HEC upon symmetrizations. By looking at analogous general-n results for arbitrary quantum states in Sec. V, we are then able to quantify the typicality of holographic entropies upon symmetrization in Sec. VI: with respect to the uniform volume measure of entropy space, the latter are exponentially rare in the number of parties. We conclude in Sec. VII with a summary of results and a discussion of open questions.

II. BASICS

A. Inequalities

Let us collect here some basic inequalities which will be useful for later reference. The simplest universal quantum inequality involves two parties and is known as subadditivity (SA). Proven by [21], for arbitrary disjoint subsystems I and J, SA reads

$$S_I + S_J \geq S_{I\cup J}. \tag{2.1}$$

This inequality holds trivially in holography. At three parties, there appears another well-known universal quantum inequality: strong subadditivity (SSA). Proven by [22], SSA for arbitrary overlapping subsystems I and J reads[1]

$$S_I + S_J \geq S_{I\cap J} + S_{I\cup J}. \tag{2.2}$$

The proof of this inequality in holography is nontrivial and was established by [23,24]. The first genuinely holographic inequality (i.e., valid in holography, but not in quantum theory) appears for three parties and is known as the monogamy of mutual information (MMI). Proven by [24,25], MMI for arbitrary disjoint subsystems I, J, and K reads

$$S_{I\cup J} + S_{I\cup K} + S_{J\cup K} \geq S_I + S_J + S_K + S_{I\cup J\cup K}. \tag{2.3}$$

B. Graphs

For any positive integer k, introduce the notation $[k] \equiv \{1, \ldots, k\}$. Let $G = (V, E)$ be an undirected graph with finite vertex set V and edge set E. We make G into a weighted graph by assigning a nonnegative weight w_e to every edge $e \in E$. Select some vertex subset $\partial V \subseteq V$ and call them *boundary vertices*. One then defines a coloring as a surjective map $b : \partial V \to [n+1]$. The elements $i \in [n+1]$ are called *parties*, and the nonempty subsets $I \subseteq [n+1]$ are called *subsystems*. Altogether, this structure defines a graph model of holographic entanglement.

Any subset $W \subseteq V$ characterizes a *cut* of G, defined by a set of cut edges $C(W) \subseteq E$ as

$$C(W) = \{(v, v') \in E : v \in W, v' \in V\backslash W\}. \tag{2.4}$$

The *cut weight* is defined as the total weight of its edges $\|C(W)\| = \sum_{e\in C(W)} w_e$. A set $W \subseteq V$ is a cut for a subsystem I if it contains precisely the boundary vertices colored by I, i.e., if $W \cap \partial V = b^{-1}(I)$. Any cut W for I with minimum cut weight $\|C(W)\|$ defines a *min-cut* for I. The min-cut weight for a subsystem I defines its *entropy* S_I via

$$S_I = \min\{\|C(W)\| : W \cap \partial V = b^{-1}(I)\}. \tag{2.5}$$

In the context of holography, the above can indeed be understood as computing the von Neumann entropy of a subsystem I of some pure holographic state on $[n+1]$ [10]. Such a pure state can be used to encode an arbitrary n-party, mixed holographic state on $[n]$. Due to its quantum mechanical role, the special party $n+1$ is thus referred to as the *purifier*. Notice in particular that (2.5) indeed reproduces the desired purification property that $S_I = S_{I^c}$ for complementary subsystems I and $I^c = [n+1]\backslash I$. For this reason, the *entropy vector* of the full graph model is defined excluding the purifier by

$$S = \{S_I : \varnothing \neq I \subseteq [n]\}, \tag{2.6}$$

where the conventional choice of ordering is by cardinality first, and then lexicographically. The set of all entropy vectors $S \in \mathbb{R}^{2^n-1}$ obtained this way defines the *holographic entropy cone* (HEC) for n parties, or HEC_n. In Appendix A, we give an example of how to compute the entropy vector from a weighted graph, and in Appendix B we present the extreme rays of the HEC_n for $n \leq 5$.

More generally, the definition of an entropy vector in (2.6) applies to any n-partite quantum system, with S_I denoting the von Neumann entropy of a subsystem $I \subseteq [n]$. If instead of holographic states one considers completely arbitrary quantum states, the resulting set of all n-party entropy vectors defines the *quantum entropy cone* (QEC) for n parties, or QEC_n [26]. Both the HEC and the QEC are convex cones,[2] and the former is additionally known to be polyhedral [10]. Consistent with the fact that holographic states define a special class of quantum states, the HEC is a subcone of the QEC [27]. In the following, we will be

[1]To clarify, this is a 3-party inequality because it involves three disjoint subsystems: $I\backslash J$, $J\backslash I$, and $I \cap J$.

[2]To be precise, it is actually only the topological closure of the latter which is a convex cone [26]. This technicality will not be important for us.

interested in studying the HEC and how it relates to the QEC.

III. SYMMETRIZATIONS

Both entropy cones of interest in this paper are clearly symmetric under permutations of the colors $[n]$. To see a larger symmetry, recall that subsystems $I \subseteq [n+1]$ obey $S_I = S_{I^c}$. Hence these entropy cones are symmetric not only under permutations of $[n]$, but also under the extended symmetric group Sym_{n+1} of permutations of $[n+1]$ involving the purifier $n+1$.

We would like to simplify the structure of our entropy cones by defining a *symmetrization*, i.e., an operation P on their elements that is invariant under the action of Sym_{n+1}. More explicitly, if x and y are two elements of an entropy cone in the same symmetry orbit, then they should have the same symmetrized form $P(x) = P(y)$. By asking that this symmetrization be a linear map, we will be guaranteed that the symmetrization of a full convex cone remain so. The symmetrized versions of the HEC and QEC will respectively be referred to as SHEC and SQEC.

For an entropy vector $S \in \mathbb{R}^{2^n-1}$, our symmetrization will be some linear map $P\colon S \mapsto \tilde{S}$. To build it, first note that by the Sym_n symmetry of permutations of $[n]$, P can only depend on the cardinality $|I|$ of the coordinate $I \subseteq [n]$. Additionally, by the full action of Sym_{n+1} on $[n+1]$ with the identification $S_{I^c} = S_I$, one has that coordinates of cardinalities $|I|$ and $|I^C| = n+1-|I|$ are also related. Altogether, this means that P should just depend on at most $\lceil n/2 \rceil$ different variables, associated to the distinct possible cardinalities of subsets of $[n+1]$ with complements identified. The codomain of P is thus $\mathbb{R}^{\lceil n/2 \rceil}$, and one can label the *symmetric variables* $\tilde{S}_k$ of the *symmetrized vector* $\tilde{S} \in \mathbb{R}^{\lceil n/2 \rceil}$ by cardinalities $1 \le k \le \lceil n/2 \rceil$. A natural way of defining P thus employs subsets of $[n+1]$ of fixed cardinality k from 1 to $\lceil n/2 \rceil$,

$$Q_n(k) = \{I \subseteq [n+1] : |I| = k\}. \tag{3.1}$$

Then the symmetric variables can be obtained by just summing over coordinates in $Q_n(k)$,

$$\tilde{S}_k = \frac{1}{|Q_n(k)|} \sum_{I \in Q_n(k)} S_I, \qquad |Q_n(k)| = \binom{n+1}{k}, \tag{3.2}$$

where we have introduced a natural normalization factor accounting for the number of terms in the sum. In other words, we can just think of $\tilde{S}_k$ as the average of all entropies over k-partite subsystems of $[n+1]$. For instance, for $n = 3$, the symmetric variables in (3.2) are

$$\begin{aligned}
\tilde{S}_1 &= \frac{1}{4}(S_1 + S_2 + S_3 + S_4) = \frac{1}{4}(S_1 + S_2 + S_3 + S_{123}),\\
\tilde{S}_2 &= \frac{1}{6}(S_{12} + S_{13} + S_{14} + S_{23} + S_{24} + S_{34})\\
&= \frac{1}{3}(S_{12} + S_{13} + S_{23}),
\end{aligned} \tag{3.3}$$

where in the last equalities we used $S_{I^c} = S_I$. Crucially, notice that these sets $Q_n(k)$ automatically take care of coordinates $I \subseteq [n]$ of cardinality $|I| = n+1-k$, since $I^C \in Q_n(k)$. Hence the operation $P\colon \mathbb{R}^{2^n-1} \to \mathbb{R}^{\lceil n/2 \rceil}$ defined this way is a valid linear symmetrization invariant under Sym_{n+1}. For any number of parties n, the SHEC and SQEC will thus be convex cones defined by the sets of all symmetrized entropy vectors $\tilde{S} \in \mathbb{R}^{\lceil n/2 \rceil}$ obtained from symmetrizations of their parent entropy vectors $S \in \mathbb{R}^{2^n-1}$ of the HEC and QEC, respectively.

In the case of the HEC, the symmetrization of entropy vectors that we just described can also be easily arrived at from a symmetrization of graph models themselves. Indeed, since weighted graphs are ultimately the object which defines the HEC, one may consider performing a symmetrization already at this level. Given a graph model G for n parties, consider all possible $(n+1)!$ graphs G^σ (some of which may be equal) obtained by permutations $\sigma \in \mathrm{Sym}_{n+1}$ of the colors $[n+1]$. If S and S^σ are respectively the entropy vectors from G and G^σ, one obviously has $S_I = S^\sigma_{\sigma(I)}$, where $\sigma(I) = \{\sigma(i) : i \in I\}$, or, equivalently, $S^\sigma_I = S_{\sigma^{-1}(I)}$. Suppose one now combines two permuted graphs in a disjoint manner or glued together by identifying all vertices of the same color in both. Either way, it is straightforward to see that the resulting graph $G^\sigma \oplus G^{\sigma'}$ yields $S^\sigma + S^{\sigma'}$ as its entropy vector. With a suggestive choice of notation, let us then define a permutation-averaged graph $\tilde{G}$ by

$$\tilde{G} = \frac{1}{(n+1)!} \bigoplus_{\sigma \in \mathrm{Sym}_{n+1}} G^\sigma, \tag{3.4}$$

where the multiplication shall be understood as rescaling the weights of the graphs. The computation of the entropy of I in this graph $\tilde{G}$ gives

$$\begin{aligned}
\frac{1}{(n+1)!} \sum_{\sigma \in \mathrm{Sym}_{n+1}} S^\sigma_I = \frac{k!(n+1-k)!}{(n+1)!} \sum_{J \in Q_n(k)} S_J = \tilde{S}_k,\\
k = \min\{|I|, n+1-|I|\},
\end{aligned} \tag{3.5}$$

which recovers precisely the symmetric variables in (3.2). In other words, the entropies of $\tilde{G}$ only depend on the cardinality of the subsystem I and are given by the entries of the symmetric entropy vector $\tilde{S}$ of the original graph G. In this sense, we see that given a graph G, the operations of symmetrization and computation of entropies commute.

Having dealt with entropy vectors, we would now like to have an analogous operation that we can directly apply to the dual vectors q which define entropy inequalities via the scalar product $qS \geq 0$. To do so, consider constructing valid inequalities that we can write down using only the symmetric variables in (3.2). This can be accomplished by, given an inequality $qS \geq 0$, adding up all inequalities in its symmetry orbit so as to form a new inequality $q'S \geq 0$ which will be valid by convexity. The coefficients of the new vector q' can be easily computed to be

$$q'_I = k!(n+1-k)! \sum_{J \in Q_n(k)} q_J, \qquad k = \min\{|I|, n+1-|I|\}, \tag{3.6}$$

where the combinatorial factor accounts for the permutations in Sym_{n+1} which fix each J. As expected, q'_I has the right dependence on cardinality only, and we can now write $q'S \geq 0$ using just $\tilde{S}_k$ variables. Declaring $q'_{I^c} = q'_I$ for convenience, one finds

$$q'S = \sum_{\varnothing \neq I \subseteq [n]} q'_I S_I = \sum_{k=1}^{\lceil n/2 \rceil} \sum_{I \in Q_k(n)} q'_I S_I = (n+1)! \sum_{k=1}^{\lceil n/2 \rceil} \tilde{q}_k \tilde{S}_k, \tag{3.7}$$

where in the last equality we have identified the desired *symmetric coefficients* of our symmetrized inequality $\tilde{q}\,\tilde{S} \geq 0$ to be

$$\tilde{q}_k = \sum_{J \in Q_n(k)} q_J. \tag{3.8}$$

One can understand this operation as a right inverse of the one in (3.2). Formally, (3.8) defines the dual isometry P^* which makes the symmetrization P into a coisometry, with PP^* the identity on $\mathbb{R}^{\lceil n/2 \rceil}$ and P^*P a projection in $\mathbb{R}^{2^n-1}$. More explicitly, let M and M^* respectively be the rectangular matrices implementing the linear maps (3.2) and (3.8) by $\tilde{S} = MS$ and $\tilde{q} = qM^*$. Then one easily verifies that M^* is the canonical Moore-Penrose right inverse of M, given by $M^T(MM^T)^{-1}$. For instance, for $n = 3$ these matrices are

$$M = \begin{bmatrix} \frac{1}{4} & \frac{1}{4} & \frac{1}{4} & 0 & 0 & 0 & \frac{1}{4} \\ 0 & 0 & 0 & \frac{1}{3} & \frac{1}{3} & \frac{1}{3} & 0 \end{bmatrix},$$
$$M^* = \begin{bmatrix} 1 & 1 & 1 & 0 & 0 & 0 & 1 \\ 0 & 0 & 0 & 1 & 1 & 1 & 0 \end{bmatrix}^T, \tag{3.9}$$

and one clearly has $MM^* = \mathbb{1}_2$. The associated projection of vectors $S \in \mathbb{R}^{2^n-1}$ onto the symmetric subspace within $\mathbb{R}^{2^n-1}$ is then given by M^*M, which is idempotent as it should be. For the $n = 3$ example above, this projection matrix reads

$$M^*M = \begin{bmatrix} \frac{1}{4} & \frac{1}{4} & \frac{1}{4} & 0 & 0 & 0 & \frac{1}{4} \\ \frac{1}{4} & \frac{1}{4} & \frac{1}{4} & 0 & 0 & 0 & \frac{1}{4} \\ \frac{1}{4} & \frac{1}{4} & \frac{1}{4} & 0 & 0 & 0 & \frac{1}{4} \\ 0 & 0 & 0 & \frac{1}{3} & \frac{1}{3} & \frac{1}{3} & 0 \\ 0 & 0 & 0 & \frac{1}{3} & \frac{1}{3} & \frac{1}{3} & 0 \\ 0 & 0 & 0 & \frac{1}{3} & \frac{1}{3} & \frac{1}{3} & 0 \\ \frac{1}{4} & \frac{1}{4} & \frac{1}{4} & 0 & 0 & 0 & \frac{1}{4} \end{bmatrix}. \tag{3.10}$$

IV. THE SYMMETRIZED HEC

Full descriptions of the HEC in terms of extreme rays and facets are known for $n \leq 5$ [10–12]. From this data, it is straightforward to compute the SHEC for $n \leq 5$ by applying (3.2) to extreme rays and (3.8) to facets (see Appendix B). One can then easily check that the resulting descriptions of the SHEC are indeed dual to each other.

At this point, one already notices that the extreme rays of the SHEC for all $n \leq 5$ can be generated by a very simple family of graphs.[3] In particular, they can all be captured by star graphs with $n+1$ edges, one for each boundary vertex, where the weight of all but one of them can be set to unity. The remaining edge, which by symmetry and without loss of generality can be picked to be the one associated to the purifier $n+1$, then carries some other integer weight $w \geq 1$, as in Fig. 1. We observe that this family of star graphs turns out to yield precisely all extreme rays at each n when the weight w is chosen to be of the same parity as n and obey $1 \leq w \leq n$. These observations lead to the following conjecture:

Conjecture 1 (SHEC extreme rays)**.** The extreme rays of the SHEC_n can be generated by star graphs with n weight-1 edges and another edge of positive weight $w = n, n-2, \ldots$

As a sanity check, notice that this proposal is consistent with the dimensionality of the SHEC, since the number of conjectured extreme rays $\lceil n/2 \rceil$ precisely matches it. In turn, this suggests that the SHEC may be a simplicial cone for all n. To be more explicit, and building upon Conjecture 1, we now work out a closed-form expression for all conjectured extreme rays of the SHEC_n. Firstly, from the star graph in Fig. 1, every entropy S_I is by definition given by

$$S_I = \min\{|I|, n - |I| + w\}. \tag{4.1}$$

Since S_I only depends on the subsystem cardinality $k = |I|$,

[3]Intuitively, by "generated" here we mean that these graphs yield entropy vectors whose symmetrizations through (3.2) match the extreme rays of the SHEC.

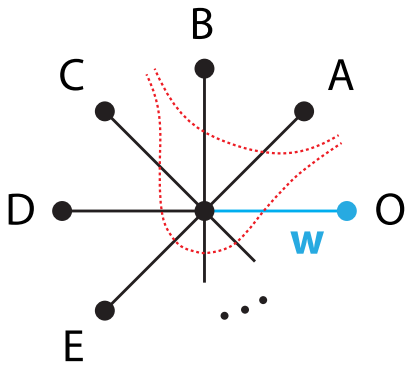

FIG. 1. General star graphs realizing the extreme rays of the SHEC. Black edges have unit weight, while the blue "purification" edge has positive integer weight. This is $w = 1, 3, \ldots, n$ for n odd, and $w = 2, 4, \ldots, n$ for n even. Dashed red lines represent the two possible min-cuts for subsystem AB. An analogous binary choice of including or excluding the central vertex exists for every subsystem.

using momentarily the notation $S_I = S_k$, it is then straightforward to apply (3.2) and obtain the coordinates of the symmetrized entropy vectors as

$$\begin{aligned}\tilde{S}_k &= \binom{n+1}{k}^{-1}\left(\binom{n}{k}S_k + \binom{n}{n+1-k}S_{n+1-k}\right)\\ &= \frac{1}{n+1}((n+1-k)\ \min\{k, n-k+w\}\\ &\quad + k\min\{n+1-k, w+k-1\}).\end{aligned} \tag{4.2}$$

The particular set of star graphs we are interested in for each n can be conveniently parametrized by setting $w = n - 2(l-1)$ for $l = 1, 2, \ldots, \lceil n/2\rceil$. This way, l labels each of the $\lceil l/2\rceil$ conjectured extreme rays, whose entropies in (4.2) can be further simplified to

$$\tilde{S}_k^{(l)} = \frac{2k}{n+1}(n+1-\max\{k,l\}). \tag{4.3}$$

We can now use this result in order to obtain explicit results for the complete set of extreme rays of the SHEC for any number of parties n according to Conjecture 1.

The $\lceil n/2\rceil$ entropy vectors of dimension $\lceil n/2\rceil$ we obtain for each n this way can be arranged as columns of a square matrix. For instance, for $n = 10$ (and with entropy vectors conveniently renormalized by a factor of $(n+1)/2$), this matrix can be written as

$$M_{10}^{\mathrm{SHEC}} = \begin{bmatrix} 10 & 9 & 8 & 7 & 6\\ 18 & 18 & 16 & 14 & 12\\ 24 & 24 & 24 & 21 & 18\\ 28 & 28 & 28 & 28 & 24\\ 30 & 30 & 30 & 30 & 30 \end{bmatrix}. \tag{4.4}$$

One can easily check that these matrices are nonsingular for every n, thereby demonstrating that the conjectured SHEC indeed is a simplicial cone of full dimension in $\mathbb{R}^{\lceil n/2\rceil}$. As such, its dual facet description can be immediately obtained from the rows of the inverse of the matrices of extreme rays just described. For the $n = 10$ example above, this leads to

$$(M_{10}^{\mathrm{SHEC}})^{-1} = \begin{bmatrix} 1 & -\frac{1}{2} & 0 & 0 & 0\\ -1 & 1 & -\frac{1}{3} & 0 & 0\\ 0 & -\frac{1}{2} & \frac{2}{3} & -\frac{1}{4} & 0\\ 0 & 0 & -\frac{1}{3} & \frac{1}{2} & -\frac{1}{5}\\ 0 & 0 & 0 & -\frac{1}{4} & \frac{7}{30} \end{bmatrix}, \tag{4.5}$$

where from e.g. the first row one reads off the inequality,

$$2\tilde{S}_1 - \tilde{S}_2 \geq 0. \tag{4.6}$$

This expression can be easily checked to come from a symmetrization of SA in (2.1) for singletons and turns out to define a facet of the conjectured SHEC for all n. For each n, there also appears a new, n-dependent inequality involving symmetrized subsystems of just two different cardinalities [cf. the last row in (4.5)],

$$-\left(1-\frac{1}{\lceil\frac{n+1}{2}\rceil}\right)^{-1}\tilde{S}_{\lceil n/2\rceil-1} + \left(1+\frac{1}{\lceil\frac{n+1}{2}\rceil}\right)\tilde{S}_{\lceil n/2\rceil} \geq 0. \tag{4.7}$$

The $n = 3$ and $n = 4$ inequalities can just be obtained from MMI symmetrized under the corresponding Sym_n. However, for higher n, (4.7) will only follow from genuinely new higher-party inequalities. Finally, the remaining set of inequalities completing the list of $\lceil n/2\rceil$ facets are captured by

$$\begin{aligned}&-l(l+1)\tilde{S}_{l-1} + 2(l-1)(l+1)\tilde{S}_l - (l-1)l\tilde{S}_{l+1} \geq 0\\ &\quad \text{for } l = 2, \ldots, \lceil n/2\rceil - 1.\end{aligned} \tag{4.8}$$

This last family can in fact be extended to $l = \lceil n/2\rceil$ in order to also reproduce (4.7) by declaring that $\tilde{S}_{\lceil n/2\rceil+1} = \tilde{S}_{\lceil n/2\rceil}$. In particular, (4.7) can be understood as just a finite-n modification of (4.8) for large subsystems of half the size of the n-partite system. This can be exemplified by MMI, which as a 3-party inequality gives (4.7) when symmetrized under Sym_n for $n \in \{3, 4\}$, but for $n \geq 5$, it yields the $l = 2$ form of (4.8). To summarize, we have the following result:

Corollary 1 (SHEC facets)**.** If Conjecture 1 holds, the facets of the SHEC_n are defined by the set of inequalities given by (4.6), (4.7), and (4.8).

Because all extreme rays in Conjecture 1 are realizable by star graphs, it follows that the conjectured SHEC is contained in the true SHEC. Whether or not Conjecture 1 is true thus depends on whether the conjectured facets of the SHEC are actually obtainable from symmetrizations of valid HEC inequalities. In other words, proving our

conjecture requires finding and proving valid HEC inequalities for arbitrary n, which is a hard problem. Our explicit knowledge of the HEC_n for small n allows us to perform some checks on the conjectured SHEC. We will be able to provide a complete proof of our conjecture for up to $n = 6$ but only a partial one for larger n.

As already mentioned, the conjectured SHEC facet (4.6) arises from singleton SA. Since this is a valid inequality of the HEC for all n, it follows that (4.6) is a valid facet of the SHEC for all n. Since (4.7) can be understood as a special case of (4.8), let us turn to the latter straightaway (see footnotes below). For $l = 2$, this yields

$$-3\tilde{S}_1 + 3\tilde{S}_2 - \tilde{S}_3 \geq 0. \tag{4.9}$$

It is a simple exercise to show that this follows from the MMI inequality in (2.3) for singletons when symmetrized for $n \geq 5$.[4] Again, since MMI is a well-known HEC inequality which holds for all n, it follows that (4.9) is a valid facet of the SHEC for all n. Further, (4.8) for $l = 3$ gives

$$-6\tilde{S}_2 + 8\tilde{S}_3 - 3\tilde{S}_4 \geq 0. \tag{4.10}$$

This inequality can be seen to arise from any one of the last three 5-party inequalities in Appendix B when symmetrized for $n \geq 7$.[5]

These results suffice to prove validity of our proposal for the extremal elements of the SHEC_n for up to $n = 6$. Unfortunately, our incomplete knowledge of the HEC_n for larger n is insufficient to do so for $n \geq 7$, for which a different approach that bypasses full knowledge of the HEC will be needed.

V. THE SYMMETRIZED QEC

The QEC is poorly understood and only known exactly for up to $n = 3$. At this number of parties, its facets belong to the two orbits associated to the following inequalities:

$$S_1 + S_2 \geq S_{12},$$
$$S_{12} + S_{23} \geq S_2 + S_{123}. \tag{5.1}$$

The first one can be recognized as the SA inequality in (2.1), while the last one corresponds to SSA as in (2.2). Going to higher n, different instances of the same type of inequality associated to inequivalent choices of subsystems can define algebraically independent orbits of inequalities. This way, one can apply SA and SSA to all possible subsystems in order to construct a rich polyhedral cone bounded by multiple orbits of these two types of inequalities. Because both are universal quantum inequalities, the resulting cone defines an outer approximation to the QEC. A neat study of precisely which of these orbits of SA and SSA constitute facets of the resulting cone, and which are redundant, was performed by Pippenger in [26].

Additionally, for arbitrary number of parties n, Pippenger studied the cone that results under Sym_n symmetrizations. More specifically, rather than symmetrizing over all $I \subseteq [n+1]$ for each $|I| = k \leq \lceil n/2 \rceil$, Pippenger considered symmetrizations only over $I \subseteq [n]$ for each $|I| = k \leq n$, thus not including the purification symmetry. Even for this milder Sym_n symmetrizations, he was able to prove that every extreme ray of the resulting cone is realizable by some quantum state.[6] This way, he established that the cone of SA and SSA instances collapses down to precisely match the QEC under respective Sym_n symmetrizations. As we did for the HEC, here we will instead consider Sym_{n+1} symmetrizations; i.e., we further symmetrize over the purifier. This symmetrization of the QEC defines the SQEC, which by [26] will of course continue to match the cone of SA and SSA instances accordingly symmetrized under Sym_{n+1}. In other words, using the results of [26], we will be able to present complete descriptions of the SQEC for all n.

Like the SHEC, the SQEC turns out to be simplicial. For each n, the facets of the SQEC are given by the following set of $\lceil n/2 \rceil$ inequalities:

$$-\tilde{S}_{l-1} + 2\tilde{S}_l - \tilde{S}_{l+1} \geq 0 \quad \text{for } 1 \leq l \leq \lceil n/2 \rceil, \tag{5.2}$$

where we have declared $\tilde{S}_0 = 0$ and $\tilde{S}_{\lceil n/2 \rceil + 1} = \tilde{S}_{\lceil n/2 \rceil}$. For $l = 1$, (5.2) yields (4.6), which recall comes from the SA facet that the QEC shares with the HEC. The rest come from symmetrizations of SSA inequalities as in (2.2) for subsystems $I, J \subseteq [n]$ obeying $|I \cap J| = 2, 3, \ldots, \lceil n/2 \rceil$.

One can easily see that the SQEC is a simplicial cone. Writing out its facet-defining vectors as rows in a matrix, the extreme rays of the SQEC can thus be obtained as the column vectors of the inverse matrix. For instance, for $n = 10$, the matrix of row inequalities reads

$$M_{10}^{\mathrm{SQEC}} = \begin{bmatrix} 2 & -1 & 0 & 0 & 0 \\ -1 & 2 & -1 & 0 & 0 \\ 0 & -1 & 2 & -1 & 0 \\ 0 & 0 & -1 & 2 & -1 \\ 0 & 0 & 0 & -1 & 1 \end{bmatrix}, \tag{5.3}$$

and its inverse of column extreme rays yields

[4] For $n = 3$ and $n = 4$, as shown in Appendix B, (4.9) respectively collapses down to $-4\tilde{S}_1 + 3\tilde{S}_2 \geq 0$ and $-3\tilde{S}_1 + 2\tilde{S}_2 \geq 0$, which take the form of (4.7) [see comment below (4.8)].

[5] As was the case for MMI in the footnote above, if symmetrized for $n = 5$ or $n = 6$, these instead give rise to the special case of (4.7) corresponding to (4.8) applied to $l = \lceil n/2 \rceil$. For $n = 5$, as shown in Appendix B, these symmetrize down to $-9\tilde{S}_2 + 8\tilde{S}_3 \geq 0$, while for $n = 6$ they give $-6\tilde{S}_2 + 5\tilde{S}_3 \geq 0$.

[6] There is a minor typo associated to Theorem 5.5 of [26]: in Eq. (5.20) therein, the condition $n - a + 1 \leq b \leq n$ should instead read $n - a \leq b \leq n$.

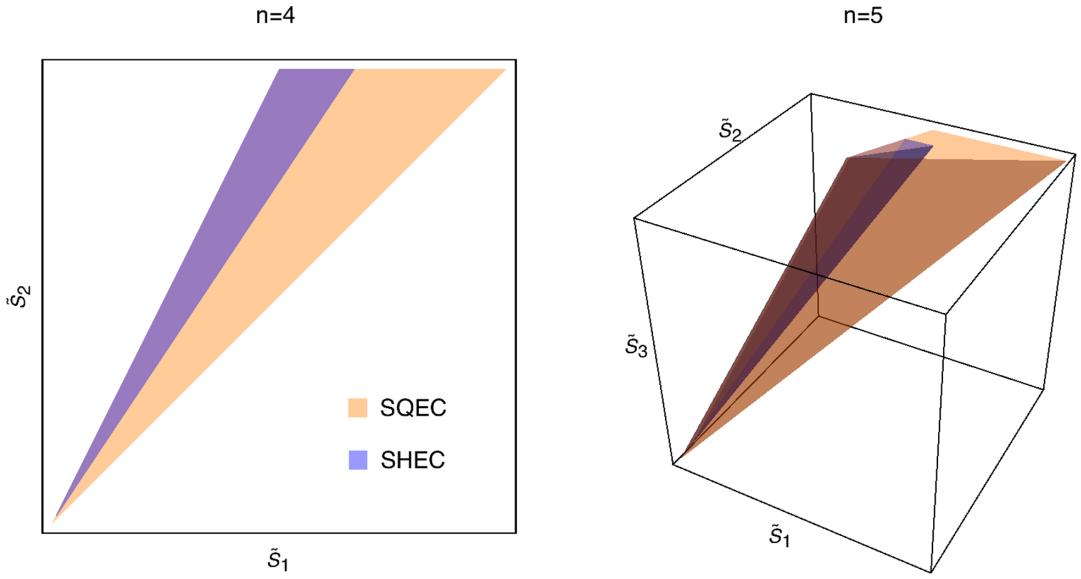

FIG. 2. The SQEC and SHEC for $n = 4, 5$.

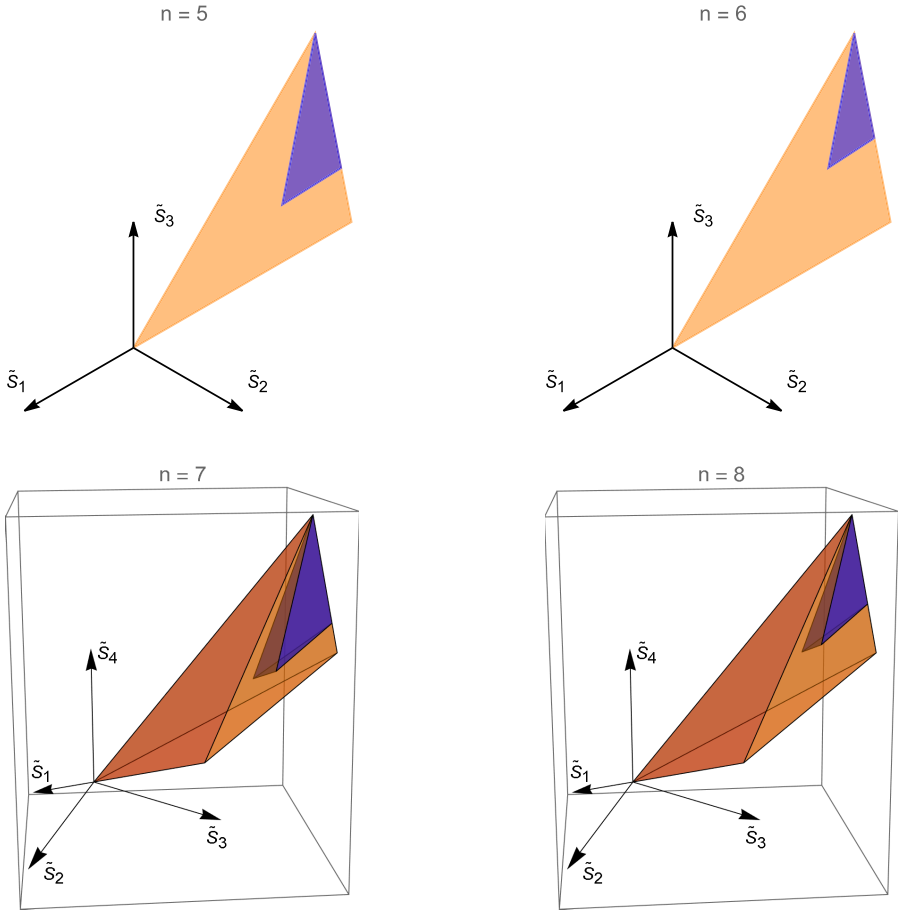

FIG. 3. Cross sections of the SQEC and SHEC through the hyperplane defined by $\sum_{k=1}^{\lceil n/2 \rceil} \tilde{S}_k = 1$ for $n = 5, 6, 7, 8$. The cross section of the positive orthant is not shown because it is too large. Instead, for orientation we show arrows pointing in the direction in which the intersections with the canonical basis vectors occur—these would define the extreme points of the positive orthant in the cross section.

$$(M_{10}^{\mathrm{SQEC}})^{-1} = \begin{bmatrix} 1 & 1 & 1 & 1 & 1 \\ 1 & 2 & 2 & 2 & 2 \\ 1 & 2 & 3 & 3 & 3 \\ 1 & 2 & 3 & 4 & 4 \\ 1 & 2 & 3 & 4 & 5 \end{bmatrix}. \tag{5.4}$$

For general n, letting $l = 1, 2, \ldots, \lceil n/2 \rceil$ enumerate each of the resulting vectors, the kth component of the lth extreme ray can be easily seen to be given by

$$\tilde{S}_k^{(l)} = \min\{k, l\}. \tag{5.5}$$

In Fig. 2, we illustrate the SQEC and SHEC full dimensionally for $n = 4$, 5. In Fig. 3, we illustrate the SQEC and SHEC via codimension-1 radial cross sections for $n = 5$, 6, 7, 8. A question naturally arising is now how these two cones relate to each other. In particular, we will be interested in comparing their "size," and the scaling with n.

VI. VOLUMES OF SYMMETRIZED ENTROPY CONES

The volume of a pointed polyhedral cone is infinite. However, if the cone lies within a small solid angle inside the positive orthant, then a useful notion of how large it is can be obtained as the volume of the polytope it forms up to some choice of cross section. When this cone is simplicial, as is the case for both the SQEC and the SHEC, this polytope is a simplex whose vertices are the origin and the intersection of its extreme rays with the cross section. The volume of such a simplex can be easily computed using the determinant of the matrix of extreme rays $\hat{M}$ suitably normalized to match the vertices on the cross section. Since the determinant actually computes the volume of the parallelotope formed by the vectors involved, one has to divide it by a combinatorial factor of $d!$ to obtain the volume of the corresponding d-dimensional simplex. Denoting a general matrix of normalized extreme rays of a d-dimensional simplicial cone by $\hat{M}$, we will thus define its volume by

$$\mathrm{vol}(\mathrm{cone}\{\hat{M}\}) \equiv \frac{1}{d!} |\det \hat{M}|. \tag{6.1}$$

When considering the SQEC and the SHEC, our starting point will be a matrix M of unnormalized, integral extreme rays. A natural choice of cross section is the hyperplane defined by $\sum_{k=1}^{\lceil n/2 \rceil} \tilde{S}_k = 1$, as in Fig. 3. The vertices on the cross section can then be easily obtained by normalizing the extreme rays of the desired cone linearly to unity, i.e., using the taxicab norm. Explicit numerical results for small n are given in Appendix D. More generally, we are interested in the scaling of volumes as $n \to \infty$. Our strategy for obtaining this will be as follows:

(1) Derive a simple general expression for the determinant of M.
(2) Derive an expression for the product $\Pi(M)$ of the norms of all extreme rays in M.
(3) Obtain the desired (normalized) determinant as $|\det \hat{M}| = \frac{|\det M|}{\Pi(M)}$.

For the SQEC_n, the extreme rays are given componentwise by (5.5), which we will take to define our unnormalized matrix of extreme rays M_n^{SQEC}. The determinant of the matrix formed by these vectors is always unity for all n, i.e., $\det M_n^{\mathrm{SQEC}} = 1$, which takes care of step 1. Letting $d_n = \lceil n/2 \rceil$ for convenience, the normalization factor $\Pi(M_n^{\mathrm{SQEC}})$ resulting from step 2 can also be obtained exactly and reads

$$\Pi(M_n^{\mathrm{SQEC}}) = \frac{(2d_n)!}{2^{d_n}}. \tag{6.2}$$

We can thus conclude that the volume of the SQEC for n parties is exactly given by

$$\mathrm{vol}(\mathrm{SQEC}_n) = \frac{1}{d_n!} \frac{2^{d_n}}{(2d_n)!}. \tag{6.3}$$

Since we will be ultimately interested only in the large-n scaling of this volume, we may consider keeping track of just the leading order behavior of (6.3) as $n \to \infty$. Undergoing numerically coarser approximations at large n, and taking n to be even (such that $d_n = n/2$), one obtains

$$\mathrm{vol}(\mathrm{SQEC}_n) \sim \frac{1}{(n/2)!} \frac{e^{\frac{13}{10}n}}{n^{\frac{1}{2}+n}} \sim \frac{e^{\frac{11}{5}n}}{n^{1+\frac{3}{2}n}}. \tag{6.4}$$

Although slightly more complicated, the same approach can be applied to the SHEC. We will use (4.3) with an $(n+1)/2$ prefactor for the unnormalized extreme rays in M_n^{SHEC}. Remarkably, the determinants of the resulting matrix are easily computable and read

$$\det M_n^{\mathrm{SHEC}} = \left\lceil \frac{n+1}{2} \right\rceil ! \times \begin{cases} 1 & \text{if } n \text{ is even}, \\ \frac{n+1}{2} & \text{if } n \text{ is odd}. \end{cases} \tag{6.5}$$

The exact result for $\Pi(M_n^{\mathrm{SHEC}})$ can be written

$$\Pi(M_n^{\mathrm{SHEC}}) = \left(-\frac{1}{6}\right)^{d_n} \prod_{k=1}^{3} (1 - x_k)_{d_n}, \tag{6.6}$$

where the subscripted brackets denote the Pochhammer symbol $(a)_k = \frac{\Gamma(a+k)}{\Gamma(a)}$, and x_k stands for the kth root of the following third-order polynomial:

$$\prod_{k=1}^{3}(x-x_k)=x^3-x-d_n(d_n+1)(3n-2(d_n-1)). \quad (6.7)$$

Albeit exact, (6.6) still relies on an implicit expression for the x_k roots. We could of course use the general formulae for the roots of a third-order polynomial, but this would not be very illuminating. Instead, we will take advantage of large-n approximations in order to get a more explicit result for this. A key observation is to notice that the roots of (6.7) scale linearly with n. Hence, to simplify this polynomial nontrivially at large n, we will first have to factor out this uninteresting n-dependence. We can do so by letting $x = d_n\hat{x}$ and introducing renormalized roots $x_k = d_n\hat{x}_k$. Plugging these into (6.7), at leading order in n we obtain

$$\prod_{k=1}^{3}(\hat{x}-\hat{x}_k)\approx\hat{x}^3-4. \quad (6.8)$$

The renormalized roots no longer depend on n and are simply the cubic roots of 4. In terms of these, we can reexpress (6.6) as

$$\Pi(M_n^{\mathrm{SHEC}})\approx\left(-\frac{1}{6}\right)^{d_n}\prod_{k=1}^{3}(1-\hat{x}_k d_n)_{d_n}, \quad (6.9)$$

and expand the Pochhammer symbols at large n. For each root, this expansion yields

$$(1-d_n\hat{x}_k)_{d_n}\approx\left(1-\frac{1}{\hat{x}_k}\right)^{\frac{1}{2}+(1-\hat{x}_k)d_n}\left(-\frac{\hat{x}_k d_n}{e}\right)^{d_n}. \quad (6.10)$$

Taking the product over all roots in (6.9) and making some numerical approximations, we arrive at

$$\Pi(M_n^{\mathrm{SHEC}})\approx\frac{\sqrt{3}}{2}\left(\frac{3}{5}\right)^{d_n}d_n^{3d_n}\sim e^{-\frac{13}{10}n}n^{\frac{3}{2}n}. \quad (6.11)$$

Having completed step 2, we finally obtain our desired expression for the volume of the SHEC at large n,

$$\mathrm{vol}(\mathrm{SHEC}_n)\sim\frac{1}{(n/2)!}\frac{e^{\frac{9}{2}n}}{n^{-1+n}}\sim\frac{e^{\frac{13}{10}n}}{n^{-\frac{1}{2}+\frac{3}{2}n}}. \quad (6.12)$$

We are finally ready to compare the asymptotic volumes of the SQEC and the SHEC. Using the expressions from (6.4) and (6.12), we obtain

$$\frac{\mathrm{vol}(\mathrm{SHEC}_n)}{\mathrm{vol}(\mathrm{SQEC}_n)}\sim n^{\frac{3}{2}}e^{-\frac{9}{10}n}. \quad (6.13)$$

We thus conclude that, in terms of volumes in entropy space, the SHEC_n constitutes an exponentially small fraction of the SQEC_n. This is particularly interesting considering that holographic states are in fact expected to be typical when randomly sampling some Hilbert space of quantum states with respect to an invariant measure on it.[7] We can also compare the volumes of these two cones to the volume of the unit simplex that the positive orthant defines. Using $n/2$ as the dimensionality at large n, the volume of this object is simply given by $1/(n/2)!$. Comparing this to (6.3), we see that the SQEC_n itself also occupies a very small fraction of the positive orthant which decreases faster than exponential as n increases.

VII. CONCLUSION AND OUTLOOK

We motivated and presented a projection of the HEC via a natural symmetrization which results in a much simpler (but still nontrivial) entropy cone: the SHEC. By inspecting its extremal elements, we were able to conjecture a full characterization of this cone for an arbitrary number of parties n in terms of both full sets of extreme rays and facet inequalities. Our proof of this proposal for the SHEC for small $n \leq 6$ was based on the known complete descriptions of the HEC for $n \leq 5$. In the future, however, since the SHEC is by construction a coarser and much simpler version of the HEC, one would hope to make progress in proving the general form of the SHEC without necessarily knowing such a description for the HEC. Indeed, already at the conjectural level, here we have provided a plausible general form of the SHEC for arbitrary n, while such an achievement for the HEC seems unattainable as of now.

For instance, the partial description of the HEC_6 known to date [13] already exhibits an unprecedented level of complexity compared to $n \leq 5$. While the HEC_5 consists of just 8 distinct orbits of facets and 19 orbits of extreme rays, the current description of the HEC_6 already involves at least 182 orbits of facets and at least 4122 orbits of extreme rays [13].[8] According to Conjecture 1 and Corollary 1, all this extremely rich structure that arises for $n \geq 6$ turns out to be symmetrized away at the level of the SHEC, which nonetheless still preserves some nontrivial properties of the HEC in the form of $\lceil n/2 \rceil$ facets and extreme rays at each n.

Symmetrizations provide an organizing principle for the complicated structure of the HEC. The usefulness of this organization is already evidenced by $n = 5$ e.g. at the level of facets, where we observe that (1) not all facets of the HEC remain facets of the SHEC, (2) those which remain facets do so in nontrivial families of multiple facets, and (3) it takes genuinely new facets of the HEC at each n to generate higher-n facets of the SHEC. Observation (1) is consistent with our expectations for the SHEC: for larger n there arise combinatorially large numbers of new orbits of facets for the HEC, but the simplicial SHEC should only

[7] We thank Bartek Czech for comments on this point.

[8] Data to date suggest that, in fact, these numbers are still highly underestimating the complexity of a complete description of the HEC_6.

involve $\lceil n/2 \rceil$ as per our conjecture. Observation (2) implies that there are distinguished families of facets of the HEC which remain "extremal" upon symmetrization. Observation (3) emphasizes the fact that the SHEC retains nontrivial information about the HEC for all n, thus stressing its usefulness as a prerequisite to understand the HEC. To elaborate further on this, let us emphasizes that none of the 182 facet orbits that we currently known of the HEC_6 happens to prove the form of the SHEC for $n = 7$—namely, none of them symmetrizes down to the $l = 4$ inequality coming from (4.8). This suggests that genuinely $n = 7$ information about the HEC may be needed to characterize the SHEC_7, and similarly for any larger n. It is also interesting to note that even though the $l = 3$ inequality coming from (4.8) can be realized by HEC_5 inequalities, there also appear new HEC_6 inequalities falling into the same family. For instance,

$$\begin{aligned} &-S_{12}-S_{13}-S_{14}-S_{25}-S_{26}-S_{35} \\ &+S_{123}+S_{124}+S_{125}+S_{126}+S_{134}+S_{135}+S_{235}+S_{256} \\ &-S_{1234}-S_{1235}-S_{1256}\geq 0, \end{aligned} \tag{7.1}$$

is a genuinely HEC_6 inequality (i.e., not obtainable as a lift from lower-n inequalities), whose symmetrization for $n \geq 7$ matches precisely (4.10) as well.

More generally, the symmetrizations studied here have proven to be useful in distilling nontrivial structure at arbitrary n for both the quantum and holographic entropy cones. Other interesting classes of quantum states and constructs have been studied in the past, which suffer from the same rapidly increasing complexity as n increases. It would be interesting to explore if, upon symmetrizations, one can gain some further knowledge about the general-n structure of the cone of stabilizer states [28], the cone of linear rank inequalities [29], the cone of hypergraph entropies [30–32], the cone of topological links [33], or even the HEC under quantum corrections from bulk matter fields [34].

ACKNOWLEDGMENTS

It is a pleasure to thank David Avis, Max Rota, and Jordi Tura for useful discussions. M. F. was supported by the Swiss National Science Foundation and by The Branco Weiss Fellowship—Society in Science, administered by the ETH Zürich. S. H. C. was supported by NSF Grant No. PHY-1801805 and UCSB during the early stages of this project, and is currently supported by NSF Grant No. PHY-2107939 and a Len DeBenedictis Graduate Fellowship.

Note added.—Recently, we became aware of [35], which applies the same projection to the HEC and obtains results consistent with ours.

APPENDIX A: EXAMPLE OF A GRAPH MODEL OF HOLOGRAPHIC ENTANGLEMENT

We explain here how to compute the entropy vector associated to a graph model. Consider the graph shown in Fig. 4 as a concrete example. This model consists of six boundary vertices, which correspond to $n = 5$ parties labeled from A to E, and to the purifier labeled by O. The unlabeled vertex at its center is the only bulk vertex, and it is radially connected to each party through a weight-1 edge, except for the one to the purifier which has weight 3.

The entropy S_I of each subsystem $I \subseteq \{A, B, C, D, E\}$ is given by the total weight of the minimum cut that separates it from all other boundary vertices, including the purifier. To find the entropy S_I we thus look at all possible cuts for I and compute their weight. Since there is only one bulk vertex, there will only be two such candidate cuts for each subsystem, corresponding to including or excluding the bulk vertex. These two possible cuts are illustrated in Fig. 4 by red lines for subsystem A, and by green lines for subsystem $ABCDE$. For A, one observes that excluding the bulk vertex (dashed, weight 1) has lower cost than including it (solid, weight 7). Hence the min-cut for A is given by the boundary vertex alone and yields $S_A = 1$ and similarly for all other 1-party entropies. For 2- and 3-party entropies, it continues to be preferable to exclude the bulk vertex from the cut, and the entropies one obtains are respectively 2 and 3. At 4 parties it turns out that both cuts have minimum weight, and the entropies take value 4. The situation changes for the 5-party subsystem $ABCDE$, for which the inclusion of the bulk vertex in the cut in fact reduces the cost (dashed, weight 3) against its exclusion (solid, weight 5), giving $S_{ABCDE} = 3$. All in all, we observe that the graph in Fig. 4 realizes an entropy vector corresponding to the extreme ray on the fifth row of the table for $n = 5$ in Appendix B.

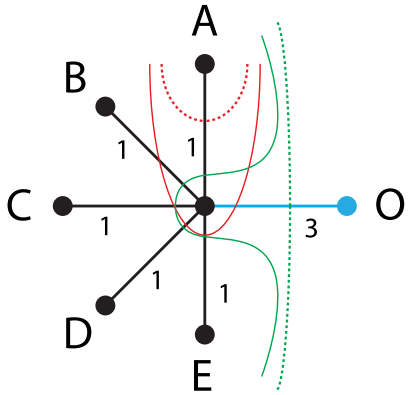

FIG. 4. Example of a graph for $n = 5$ parties. Boundary vertices are labeled by $\{A, \ldots, E\}$, and O denotes the purifier. Cuts for subsystems A and $ABCDE$ are represented by red and green lines, respectively, with min-cuts dashed.

APPENDIX B: EXTREMAL STRUCTURE OF THE SHEC FOR $n \leq 5$

The HEC has been completely characterized for $n \leq 5$ [10–12], while for larger n only partial results are known due to its rapidly increasing complexity [13]. We list here all the extreme rays and facets of the HEC for $n \leq 5$, and compute their symetrization according to the prescription presented in Sec. III.

1. Extreme rays

In the tables below, the column "Extremal?" refers to whether the symmetrized ray is extremal for the associated SHEC, while the column "w" indicates the weight of the purification edge in the star graph realizing the corresponding ray (see Fig. 1).

$n = 2$

No.	HEC	SHEC	Extremal?	w
1	(11; 0)	(1)	Yes	Any

$n = 3$

No.	HEC	SHEC	Extremal?	w
1	(110; 011; 0)	(3 4)	Yes	3
2	(111; 222; 1)	(1 2)	Yes	1

$n = 4$

No.	HEC	SHEC	Extremal?	w
1	(1100; 011110; 0011; 0)	(2 3)	Yes	4
2	(1110; 221211; 1222; 1)	(1 2)	Yes	2
3	(1111; 222222; 3333; 2)	(1 2)	Yes	2

$n = 5$

No.	HEC	SHEC	Extremal?	w
1	(11000; 0111111000; 0001111110; 00011; 0)	(5 8 9)	Yes	5
2	(11110; 2221221211; 1121221222; 01111; 0)	(5 10 12)		
3	(11112; 2223223233; 3323223222; 21111; 0)	(5 10 12)		
4	(11111; 2222222222; 3333333333; 22222; 1)	(1 2 3)	Yes	1
5	(11111; 2222222222; 3333333333; 44444; 3)	(4 8 9)	Yes	3
6	(11112; 2223223233; 3343443444; 43333; 2)	(10 20 27)		
7	(11122; 2233233334; 3444454455; 55444; 3)	(25 50 63)		
8	(11111; 2222222222; 3333333331; 22222; 1)	(5 10 14)		
9	(11112; 2223223233; 3343443442; 43333; 2)	(20 40 51)		
10	(11111; 2222222222; 2333332332; 22222; 1)	(10 20 27)		
11	(11222; 2333333444; 4445535354; 44433; 2)	(25 50 63)		
12	(11111; 2222222222; 3323323232; 22222; 1)	(5 10 13)		
13	(11111; 2222222222; 3233333232; 22222; 1)	(10 20 27)		
14	(22223; 4445445455; 6476776575; 65555; 3)	(7 14 18)		
15	(33333; 6666666666; 7759779999; 66666; 3)	(5 10 13)		
16	(11111; 2222222222; 3322332233; 22222; 1)	(5 10 13)		
17	(22223; 4445445455; 4656756777; 65555; 3)	(7 14 18)		
18	(33333; 6666666666; 5979977997; 66666; 3)	(5 10 13)		
19	(33333; 6666666666; 7957979997; 66666; 3)	(5 10 13)		

2. Facets

Below, the table entry "Facet?" refers to whether the symmetrized inequality is nonredundant for the associated SHEC.

$n = 2$

No.	HEC	SHEC	Facet?
1	$S_A + S_B - S_{AB} \geq 0$	$\tilde{S}_1 \geq 0$	Yes

$n = 3$

No.	HEC	SHEC	Facet?
1	$S_A + S_B - S_{AB} \geq 0$	$2\tilde{S}_1 - \tilde{S}_2 \geq 0$	Yes
2	$S_{AB} + S_{AC} + S_{BC} - S_A - S_B - S_C - S_{ABC} \geq 0$	$-4\tilde{S}_1 + 3\tilde{S}_2 \geq 0$	Yes

$n = 4$

No.	HEC	SHEC	Facet?
1	$S_A + S_B - S_{AB} \geq 0$	$2\tilde{S}_1 - \tilde{S}_2 \geq 0$	Yes
2	$S_{AB} + S_{AC} + S_{BC} - S_A - S_B - S_C - S_{ABC} \geq 0$	$-3\tilde{S}_1 + 2\tilde{S}_2 \geq 0$	Yes

$n = 5$

No.	HEC	SHEC	Facet?
1	$S_A + S_B - S_{AB} \geq 0$	$2\tilde{S}_1 - \tilde{S}_2 \geq 0$	Yes
2	$S_{AB} + S_{AC} + S_{BC} - S_A - S_B - S_C - S_{ABC} \geq 0$	$-3\tilde{S}_1 + 3\tilde{S}_2 - \tilde{S}_3 \geq 0$	Yes
3	$S_{AB} + S_{ACD} + S_{BCD} - S_A - S_B - S_{CD} - S_{ABCD} \geq 0$	$-2\tilde{S}_1 - \tilde{S}_2 + 2\tilde{S}_3 \geq 0$	
4	$S_{AD} + S_{BC} + S_{ABE} + S_{ACE} + S_{ADE} + S_{BDE} + S_{CDE} - S_A - S_B - S_C - S_D - S_{AE} - S_{DE} - S_{BCE} - S_{ABDE} - S_{ACDE} \geq 0$	$-2\tilde{S}_1 - \tilde{S}_2 + 2\tilde{S}_3 \geq 0$	
5	$S_{ABC} + S_{BCD} + S_{CDE} + S_{ADE} + S_{ABE} - S_{AB} - S_{BC} - S_{CD} - S_{DE} - S_{AE} - S_{ABCDE} \geq 0$	$-\tilde{S}_1 - 5\tilde{S}_2 + 5\tilde{S}_3 \geq 0$	
6	$2S_{ABC} + S_{ABD} + S_{ABE} + S_{ACD} + S_{ADE} + S_{BCE} + S_{BDE} - S_{AB} - S_{AC} - S_{AD} - S_{BC} - S_{BE} - S_{DE} - S_{ABCD} - S_{ABCE} - S_{ABDE} \geq 0$	$-9\tilde{S}_2 + 8\tilde{S}_3 \geq 0$	Yes
7	$S_{ABC} + S_{ABD} + S_{ABE} + S_{ACD} + S_{ACE} + S_{ADE} + S_{BCE} + S_{BDE} + S_{CDE} - S_{AB} - S_{AC} - S_{AD} - S_{BE} - S_{CE} - S_{DE} - S_{BCD} - S_{ABCE} - S_{ABDE} - S_{ACDE} \geq 0$	$-9\tilde{S}_2 + 8\tilde{S}_3 \geq 0$	Yes
8	$3S_{ABC} + 3S_{ABD} + 3S_{ACE} + S_{ABE} + S_{ACD} + S_{ADE} + S_{BCD} + S_{BCE} + S_{BDE} + S_{CDE} - S_{AD} - S_{AE} - S_{BC} - S_{DE} - S_{ABDE} - S_{ACDE} - 2S_{AB} - 2S_{AC} - 2S_{BD} - 2S_{CE} - 2S_{ABCD} - 2S_{ABCE} \geq 0$	$-9\tilde{S}_2 + 8\tilde{S}_3 \geq 0$	Yes

APPENDIX C: EXTREMAL STRUCTURE OF THE SQEC FOR $n \leq 5$

The extreme rays of the SQEC are very simple and given by (5.5). In contrast, the extreme rays of its parent cone defined by all possible instances of SA and SSA turn out to be extremely complicated (e.g. there are millions of them for $n = 5$). Hence we have decided to not include this data. Instead, we list here explicitly only the facets of the cone involving instances of SA and SSA and their symmetrizations, indicating which of the latter yield facets of the SQEC.

$n = 2$

No.	SA + SSA	SQEC	Facet?
1	$S_A + S_B - S_{AB} \geq 0$	$\tilde{S}_1 \geq 0$	Yes

$n = 3$

No.	SA + SSA	SQEC	Facet?
1	$S_A + S_B - S_{AB} \geq 0$	$2\tilde{S}_1 - \tilde{S}_2 \geq 0$	Yes
2	$S_A - S_B + S_{AB} \geq 0$	$\tilde{S}_2 \geq 0$	
3	$S_{AC} + S_{BC} + S_C - S_{ABC} \geq 0$	$-\tilde{S}_1 + \tilde{S}_2 \geq 0$	Yes

$n = 4$

No.	SA + SSA	SQEC	Facet?
1	$S_A + S_B - S_{AB} \geq 0$	$2\tilde{S}_1 - \tilde{S}_2 \geq 0$	Yes
2	$S_A - S_B + S_{AB} \geq 0$	$\tilde{S}_2 \geq 0$	
3	$S_A + S_{BC} - S_{ABC} \geq 0$	$\tilde{S}_1 \geq 0$	
4	$-S_A + S_{BC} + S_{ABC} \geq 0$	$-\tilde{S}_1 + 2\tilde{S}_2 \geq 0$	
5	$S_{AC} + S_{BC} - S_C - S_{ABC} \geq 0$	$-\tilde{S}_1 + \tilde{S}_2 \geq 0$	Yes

$n = 5$

No.	SA + SSA	SQEC	Facet?
1	$S_A + S_B - S_{AB} \geq 0$	$2\tilde{S}_1 - \tilde{S}_2 \geq 0$	Yes
2	$S_A - S_B + S_{AB} \geq 0$	$\tilde{S}_2 \geq 0$	
3	$S_A + S_{BC} - S_{ABC} \geq 0$	$\tilde{S}_1 + \tilde{S}_2 - \tilde{S}_3 \geq 0$	
4	$S_A - S_{BC} + S_{ABC} \geq 0$	$\tilde{S}_1 - \tilde{S}_2 + \tilde{S}_3 \geq 0$	
5	$-S_A + S_{BC} + S_{ABC} \geq 0$	$-\tilde{S}_1 + \tilde{S}_2 + \tilde{S}_3 \geq 0$	
6	$-S_C + S_{BC} + S_{AC} - S_{ABC} \geq 0$	$-\tilde{S}_1 + 2\tilde{S}_2 - \tilde{S}_3 \geq 0$	Yes
7	$-S_A - S_B + S_{AC} + S_{BC} \geq 0$	$-\tilde{S}_1 + \tilde{S}_2 \geq 0$	
8	$-S_D + S_{CD} + S_{ABD} - S_{ABCD} \geq 0$	$-\tilde{S}_1 + \tilde{S}_3 \geq 0$	
9	$-S_{CD} + S_{BCD} + S_{ACD} - S_{ABCD} \geq 0$	$-\tilde{S}_2 + \tilde{S}_3 \geq 0$	Yes

APPENDIX D: EXACT VOLUMES FOR SMALL n

From the extreme rays of the SHEC and SQEC we can compute the volume of these cones as explained in Sec. VI. For small number of parties n, this volume can be easily computed exactly. In Fig. 5, and in the following table, we show the exact relative volume between the two cones for $n \leq 10$. Note that the SHEC becomes exponentially small compared to the SQEC as n increases, see (6.13).

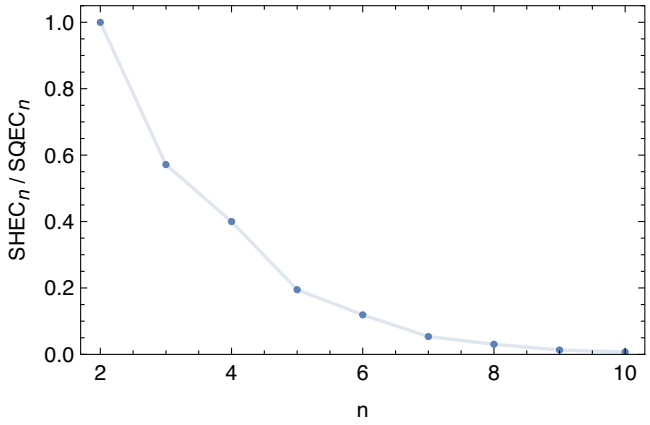

FIG. 5. Exact ratio between the volumes of the SHEC_n and SQEC_n for $2 \leq n \leq 10$.

n	2	3	4	5	6	7	8	9	10
$(\mathrm{vol}\,\mathrm{SHEC}_n)^{-1}$	1	21	30	2772	4536	1127000	1982400	1036103250	1906410000
$(\mathrm{vol}\,\mathrm{SQEC}_n)^{-1}$	1	12	12	540	540	60480	60480	13608000	13608000
$\mathrm{SHEC}_n/\mathrm{SQEC}_n$	1	0.571	0.4	0.195	0.119	0.0537	0.0305	0.0131	0.00714

[1] G. 't Hooft, Dimensional reduction in quantum gravity, Conf. Proc. C **930308**, 284 (1993), https://inspirehep.net/literature/36137.

[2] L. Susskind, The world as a hologram, J. Math. Phys. (N.Y.) **36**, 6377 (1995).

[3] J. M. Maldacena, The large N limit of superconformal field theories and supergravity, Int. J. Theor. Phys. **38**, 1113 (1999).

[4] E. Witten, Anti-de Sitter space and holography, Adv. Theor. Math. Phys. **2**, 253 (1998).

[5] M. Van Raamsdonk, Building up spacetime with quantum entanglement, Gen. Relativ. Gravit. **42**, 2323 (2010).

[6] S. Ryu and T. Takayanagi, Holographic Derivation of Entanglement Entropy from AdS/CFT, Phys. Rev. Lett. **96**, 181602 (2006).

[7] V. E. Hubeny, M. Rangamani, and T. Takayanagi, A covariant holographic entanglement entropy proposal, J. High Energy Phys. 07 (2007) 062.

[8] T. Faulkner, A. Lewkowycz, and J. Maldacena, Quantum corrections to holographic entanglement entropy, J. High Energy Phys. 11 (2013) 074.

[9] N. Engelhardt and A. C. Wall, Quantum extremal surfaces: Holographic entanglement entropy beyond the classical regime, J. High Energy Phys. 01 (2015) 073.

[10] N. Bao, S. Nezami, H. Ooguri, B. Stoica, J. Sully, and M. Walter, The holographic entropy cone, J. High Energy Phys. 09 (2015) 130.

[11] D. Avis and S. Hernández-Cuenca, On the foundations and extremal structure of the holographic entropy cone, arXiv:2102.07535.

[12] S. Hernández-Cuenca, The holographic entropy cone for five regions, Phys. Rev. D **100**, 026004 (2019).

[13] D. Avis and S. Hernández-Cuenca, The six-party holographic entropy cone (to be published).

[14] V. E. Hubeny, M. Rangamani, and M. Rota, Holographic entropy relations, Fortschr. Phys. **66**, 1800067 (2018).

[15] V. E. Hubeny, M. Rangamani, and M. Rota, The holographic entropy arrangement, Fortschr. Phys. **67**, 1900011 (2019).
[16] S. Hernández-Cuenca, V. E. Hubeny, M. Rangamani, and M. Rota, The quantum marginal independence problem, arXiv:1912.01041.
[17] T. He, M. Headrick, and V. E. Hubeny, Holographic entropy relations repackaged, J. High Energy Phys. 10 (2019) 118.
[18] T. He, V. E. Hubeny, and M. Rangamani, Superbalance of holographic entropy inequalities, J. High Energy Phys. 07 (2020) 245.
[19] J. Tura, R. Augusiak, A. B. Sainz, T. Vértesi, M. Lewenstein, and A. Acín, Detecting nonlocality in many-body quantum states, Science **344**, 1256 (2014).
[20] M. Fadel and J. Tura, Bounding the Set of Classical Correlations of a Many-Body System, Phys. Rev. Lett. **119**, 230402 (2017).
[21] O. E. Lanford III and D. W. Robinson, Mean entropy of states in quantum-statistical mechanics, J. Math. Phys. (N.Y.) **9**, 1120 (1968).
[22] E. H. Lieb and M. B. Ruskai, Proof of the strong subadditivity of quantum-mechanical entropy, Les rencontres physiciens-mathématiciens de Strasbourg-RCP25 **19**, 36 (1973), https://inspirehep.net/literature/86886.
[23] M. Headrick and T. Takayanagi, A holographic proof of the strong subadditivity of entanglement entropy, Phys. Rev. D **76**, 106013 (2007).
[24] A. C. Wall, Maximin surfaces, and the strong subadditivity of the covariant holographic entanglement entropy, Classical Quantum Gravity **31**, 225007 (2014).
[25] P. Hayden, M. Headrick, and A. Maloney, Holographic mutual information is monogamous, Phys. Rev. D **87**, 046003 (2013).
[26] N. Pippenger, The inequalities of quantum information theory, IEEE Trans. Inf. Theory **49**, 773 (2003).
[27] S. Nezami and M. Walter, Multipartite Entanglement in Stabilizer Tensor Networks, Phys. Rev. Lett. **125**, 241602 (2020).
[28] N. Linden, F. Matúš, M. B. Ruskai, and A. Winter, The quantum entropy cone of stabiliser states, LIPIcs **22**, 270 (2013).
[29] R. Dougherty, C. F. Freiling, and K. Zeger, Linear rank inequalities on five or more variables, arXiv:0910.0284.
[30] N. Bao, N. Cheng, S. Hernández-Cuenca, and V. P. Su, The quantum entropy cone of hypergraphs, SciPost Phys. **9**, 067 (2020).
[31] M. Walter and F. Witteveen, Hypergraph min-cuts from quantum entropies, J. Math. Phys. (N.Y.) **62**, 092203 (2021).
[32] N. Bao, N. Cheng, S. Hernández-Cuenca, and V. P. Su, A gap between the hypergraph and stabilizer entropy cones, arXiv:2006.16292.
[33] N. Bao, N. Cheng, S. Hernández-Cuenca, and V. P. Su, Topological link models of multipartite entanglement, arXiv:2109.01150.
[34] C. Akers, S. Hernández-Cuenca, and P. Rath, Quantum extremal surfaces and the holographic entropy cone, J. High Energy Phys. 11 (2021) 177.
[35] B. Czech and S. Shuai, Holographic cone of average entropies, arXiv:2112.00763.